J Mater Sci (2009) 44:5877–5884
DOI 10.1007/s10853-009-3830-z

Melt-processable acrylonitrile–methyl acrylate copolymers and melt-spun fibers containing MicroPCMs

Xi-yin Gao · Na Han · Xing-xiang Zhang · Wan-yong Yu

Received: 29 March 2009 / Accepted: 21 August 2009 / Published online: 1 September 2009

Abstract Acrylonitrile–methyl acrylate (AN–MA molar ratio 85/15) copolymer and copolymers containing 5–25 wt% of microencapsulated phase change materials (MicroPCMs) were synthesized by aqueous redox initiated polymerization. MicroPCMs were incorporated into the copolymer at the step of polymerization. The copolymers were processed by environment friendly, solvent-free melt-spinning. The structures and properties of the copolymers and as-spun fibers containing MicroPCMs were characterized by Nuclear Magnetic Resonance (^{1}H NMR), Gel Permeation Chromatography (GPC), Fourier Transform Infrared Spectroscopy (FTIR), Differential Scanning Calorimetry (DSC), Thermogravimetric Analysis (TG), Scanning Electronic Microscope (SEM), X-ray Diffraction (XRD), and Melting Index (MI). The results show that the composition of AN–MA copolymer agrees well with the feeding ratio of AN and MA. The copolymers containing MicroPCMs can be processed at 200 °C. The crystalline enthalpies of the fibers containing 20 and 25 wt% of MicroPCMs are 21 and 25 J/g, respectively; and they increase steadily as the contents of MicroPCMs increase. Tensile strengths of the as-spun fibers are in the range of 1.0–3.2 cN/dtex. The fibers are potentially used as raw materials to fabricate thermo-regulated fabric for comfort clothing.

X. Gao · N. Han · X. Zhang (✉) · W. Yu
Tianjin Municipal Key Lab of Fiber Modification and Functional Fiber, Institute of Functional Fibers, Tianjin Polytechnic University, Tianjin 300160, China
e-mail: zhangpolyu@yahoo.com.cn

X. Gao
e-mail: gaoxiyin6668@163.com

Introduction

Phase change materials (PCMs) can store and release latent heat during their phase transition at a defined temperature range, which can be used as thermal storage materials [1, 2]. Microencapsulation of phase change materials makes PCMs solidify permanently in the phase change procedure. Currently, MicroPCMs are incorporated into acrylic fiber, polyurethane foams or embedding into a coating compound [3–5].

Amongst, the techniques to embed MicroPCMs into the fibers by spinning were primarily studied by Bryant and Colvin who invented a fiber with integral microcapsules filled with PCMs or plastic crystals in 1988 [6]. The wet-spun polyacrylonitrile (PAN) fibers which contain 7 wt% of MicroPCMs have been put onto market since 1997 [3]. The thermo-regulated fibers have been used as the raw materials of jacket liners, long underwear, sleeping bags, and socks, etc. However, there are a number of disadvantages associated with the wet spinning, which include solvent toxicity, solvent recovery, and higher processing costs. So many researches have focused on the melt-spun fibers containing MicroPCMs [7, 8].

Melt-spun poly(butylene terephthalate) fibers containing MicroPCMs were investigated, however, the maximum content of MicroPCMs was only 3 wt% [7]; and their structures and properties were not disclosed. MicroPCMs were mixed with polyethylene and melt spun into bi-component composite fiber [8], however, the efficiency of melting enthalpy (the ratio of measured enthalpy/theoretical enthalpy) was only approximately 43%. There are still many tough problems in the evenly distribution of MicroPCMs in the polymer matrix in melt-spun process [8]. MicroPCMs are usually synthesized in water solution [9],

however, they aggregate in the process of drying. The aggregated microcapsules are destroyed in the spinning process [8, 10], or removed from the blend in the spinning process by the filter. If MicroPCMs are added in the polymerization process using water as solvent, the ratio of the aggregated microcapsules will be decreased. The energy storage properties of the polymer will be strengthened.

The approach of melt-spun PAN-based fiber containing MicroPCMs has never been reported. Because the melting temperature (T_m) of PAN (T_m, ~ 320 °C [11]) is well above its decomposition temperature, at which the polymer transforms into an insoluble, cross-linked ladder-type material, leading to the melt-spinning infeasible industrially [12]. Usually, a comonomer such as MA, acrylamide (AM), or vinyl acetate (VAc) is used to improve the solubility, spin-ability, and draw-ability [13–15]. According to the literature and our previous study [12–16], MA is found to be suitable for enabling the melt processing of PAN and the optimum MA content in the copolymer is 15 mol%.

Various contents of MicroPCMs were incorporated at the step of polymerization and the feed molar ratio of AN and MA was kept at 85/15 in the present study. Structures and properties of copolymers and as-spun fibers containing MicroPCMs were investigated.

Experimental

Materials

Acrylonitrile (AN) was obtained from Shanghai San Ai Si Reagent. Methyl acrylate (MA) was purchased from Shanghai Hua Qi (Shanghai, China). AN and MA were purified by removing inhibitor using atmospheric distillation, prior to use. Chain Transfer agent dodecyl mercaptan (RSH), was a product of Shanghai Qingpu synthetic reagent plant. Water-soluble redox initiator, potassium persulphate (KSP), was purchased from Medicament Company in China and sodium bisulphate (SBS) was a product of Hubei Province Medicament Company. MicroPCMs were prepared in our laboratory. *n*-Octadecane was used as PCM. The diameters of MicroPCMs were in the range of 0.2–3 μm. The maximum thermal resistant temperature of the microcapsules was approximately 270 °C [17].

Copolymer synthesis

The copolymer was fabricated by aqueous redox initiated polymerization; and an example of typical procedure for AN–MA 85/15 (the abbreviation AN–MA 85/15 refers to the molar feed ratio of AN and MA) was given in detail as follows.

Table 1 Weights and contents of MicroPCMs in the copolymerization

Sample no.	A	B	C	D	E
Weight of MicroPCMs (g)	0.9	1.8	2.7	3.5	4.4
Content of MicroPCMs (wt%)	5.1	10.2	15.3	19.8	24.9

A 500 mL reaction flask fitted with a condenser, stirrer and nitrogen inlet tube was charged with 250 mL of de-ionized water and purged with dry nitrogen for 30 min while heating to the reaction temperature (30 °C). The mixture of 163.5 mmol AN, 28.5 mmol MA, 1 mmol mercaptan was then added followed by 2.10 g (20.2 mmol) of the sodium bisulphite (SBS) in 5 mL de-ionized. After 5 min, 2.17 g (8 mmol) of the potassium persulphate (KSP) dissolved in 25 mL de-ionized water was added. The remaining monomer mixture (163.5 mmol AN, 28.5 mmol MA) was added over a period of 2 h. And then, an extra quantity of initiator (2.10 g of SBS in 5 mL de-ionized, 2.17 g of KSP in 25 mL de-ionized water) and a predetermined amount of MicroPCMs were added (Table 1). The admixture was held at 30 °C for an additional 1 h. The product was then directly filtered and washed with large amounts of de-ionized water and dried under vacuum at 70 °C till its weight was constant. The yields of the copolymers were in the range of 80–85%.

Melt-spinning

The fibers were melt-spun at 200 °C using a spinning machine; and the winding rate was controlled at 150 m/min.

Characterization

FTIR spectra were measured by using a spectrophotometer (BRUKER TENSOR37) at wavenumber of 400–4000 cm^{-1}.

^1H NMR spectra were obtained with a spectrometer (BRUKER AVANCE AV 300 MHz) using DMSO-d_6 as solvent.

Molecular weight measurements from gel permeation chromatography (GPC) were conducted at 50 °C with a Water M_{32} Separation Module, equipped with a Waters 410 differential refractometer detector and a Waters 510 chromatography pump coupled in parallel. DMF and polystyrene were used as solvent and standard, respectively.

The glass transition temperature (T_g) and decomposition temperature (T_d) of the copolymers were evaluated by using a differential scanning calorimeter (DSC, NETZSCH DSC 200 F3) in a nitrogen atmosphere at a heating rate of 10 °C/min.

The thermal resistant temperatures were obtained by using a thermogravimetric analysis (TG, NETZSCH, STA409 PC/PG TG-DTA) at a heating rate of 10 °C/min in a nitrogen atmosphere.

The Melting Index (MI) of the copolymers was measured in a Melting Index Tester (Chengde Tester Company, China, XNR-400A), measured at 200 °C, cylinder diameter 2.095 mm, load 5000 g.

The micrographs of the fibers were obtained by using a scanning electronic microscope (SEM, Quanta200). The fibers were broken in liquid nitrogen bath and gold-coated.

The X-ray diffraction patterns of the fibers were obtained by using X-ray diffraction (WAXD, Bruker Aux D8 Advance), 40 kV, 40 mA, Cu K_α ($\lambda = 1.5418$ Å) at room temperature, with a scanning range of 5°–40° (2θ).

The physical mechanical properties of the fibers were obtained by using a tensile strength tester (Lai Zhou Instrument Company, China, LLY-06) at a rate of 10 mm/min.

Results and discussion

Fabrication and composition of copolymers containing MicroPCMs

FTIR spectra of MicroPCMs and the copolymers containing various contents of MicroPCMs are presented in Fig. 1. The vertical coordinate of Fig. 1 has been translated.

The strong absorption peak at ~ 1734 cm^{-1} in the spectra is associated with the carboxide group (C=O) stretching vibration. The absorption peak at ~ 1204 cm^{-1} is associated with C–O group and C–N group stretching vibration, further confirming the copolymer structure.

A representative FTIR spectrum of MicroPCMs is shown as curve G. The strong multiple absorption peaks at ~ 2900 cm^{-1} are associated with saturated C–H group stretching vibration, which are the characteristic peak of *n*-octadecane. It is observed that there are also multiple peaks at ~ 2900 cm^{-1}, and which indicates that MicroPCMs exist in AN–MA matrix, on the spectra of copolymers containing MicroPCMs.

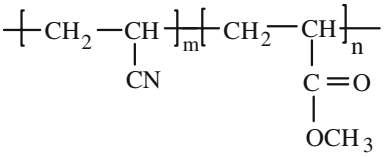

Chemical structure of AN-MA 85/15 copolymer

^{1}H NMR spectrum of AN–MA(85/15) copolymer is presented in Fig. 2. The signal at δ 3.7 corresponds to –O–CH_3; and the signal at around δ 2.0 corresponds to –CH_2–. The ratio of integrations of the –CH_3– and the –CH_2– in the copolymer (shown as A and B, respectively, in Fig. 2) was used to calculate the compositions [13, 14]. The calculated molar ratio of AN and MA is 85.38/14.62. The molar ratio of AN and MA in the copolymer agrees well with the monomer feed composition.

Molecular weight of copolymer and its distribution

The molecular weight and its distribution are shown in Fig. 3. The number average molecular weight and weight average molecular weight of the copolymer are 53,597 (M_n) and 109,467 (M_w), respectively. The dispersion index of molecular weight of AN–MA (85/15) copolymer is

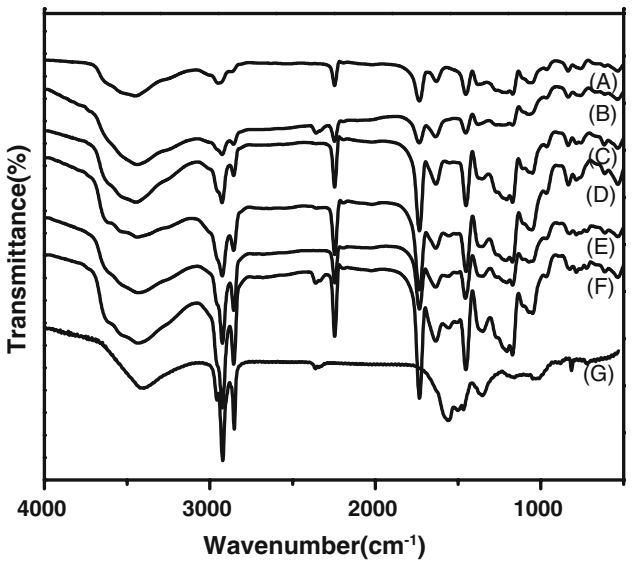

Fig. 1 FTIR spectra of MicroPCMs and copolymers containing various contents of MicroPCMs: (*A* 0 wt%, *B* 5.1 wt%, *C* 10.2 wt%, *D* 15.3 wt%, *E* 19.8 wt%, *F* 24.9 wt%, *G* MicroPCMs)

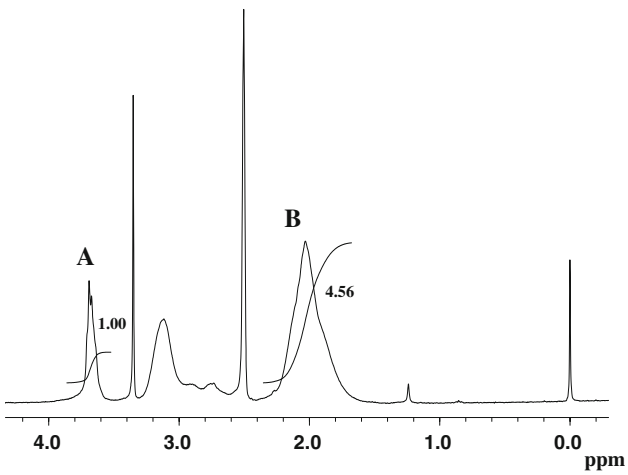

Fig. 2 ^{1}H NMR spectrum of AN–MA 85/15 copolymer

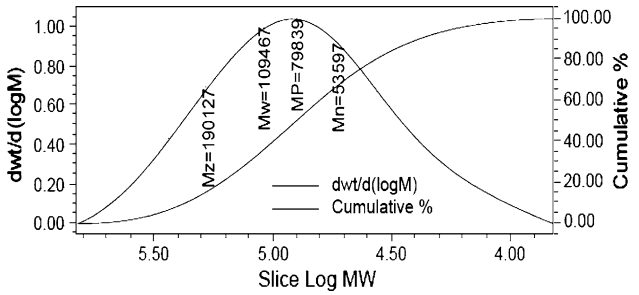

Fig. 3 GPC molecular weight and its distribution of AN–MA 85/15 copolymer

about 2.0, which is lower than that of literature [16]. The narrow molecular weight distribution is beneficial to spinning of the copolymer.

Thermal properties of the copolymers

The glass transition temperatures are shown in Fig. 4. The vertical coordinate of Fig. 4 has been translated. T_g determined by using DSC varies from 88.4 to 91.7 °C, which increases with the increase of the content of MicroPCMs (Table 2). It is possible that the PCM in MicroPCMs absorb a certain amount of heat and melt at about 30–40 °C, which is lower than the T_g onset of 85/15 AN/MA copolymer, inducing the molecular chain of AN/MA start to defreeze at a higher temperature. Besides, the entanglement of microcapsules with the molecular chains will block the remotion of molecular segments. The samples decomposition process as measured by DSC appears as a strong exothermic peak in Fig. 5. The vertical coordinate of Fig. 5 has been translated. The decomposition temperatures and decomposition enthalpies are listed in Table 2. The onset and peak decomposition temperatures of the copolymers containing MicroPCMs are lower than that of AN–MA (85/15) copolymer. It is explained as that the breakdown of MicroPCMs and the release of *n*-octadecane at high temperature accelerate the decomposition of the copolymers [18].

TG curves of the copolymers measured in the nitrogen atmosphere are presented in Fig. 6. The vertical coordinate of Fig. 6 has been translated. The thermal stable

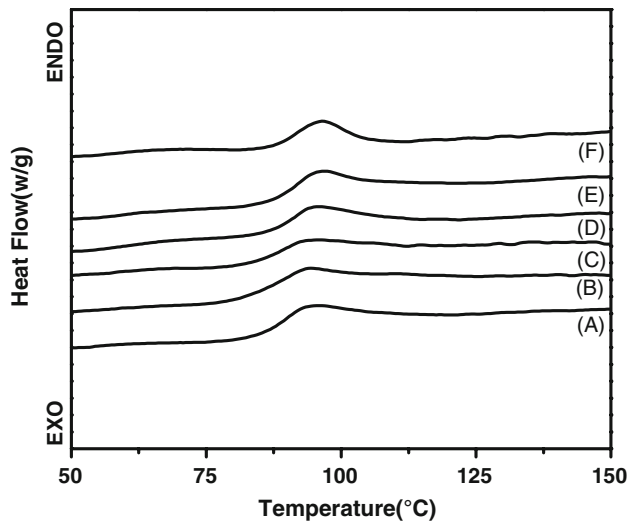

Fig. 4 DSC curves of the copolymers containing MicroPCMs depicting T_g

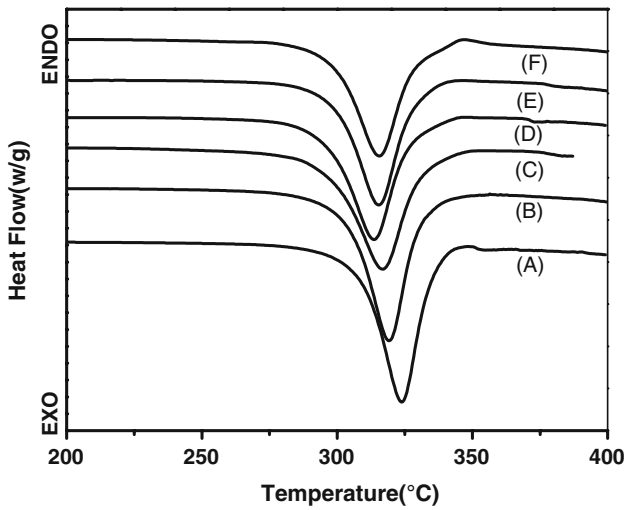

Fig. 5 DSC curves of the copolymers containing MicroPCMs depicting decomposition

Table 2 Glass transition and decomposition temperatures of the copolymers

Sample no.	Content of MicroPCMs (wt%)	T_g (°C)	T_{do} (°C)	T_{dp} (°C)	ΔH_d (J/g)
A	0	88.4	308.5	323.9	527
B	5.1	88.5	303.5	319.2	522
C	10.2	89.1	296.8	316.8	539
D	15.3	91.0	295.8	313.6	503
E	19.8	91.3	298.7	315.4	473
F	24.9	91.7	298.2	315.7	482

T_g glass transition temperature, T_{do} decomposition onset temperature; T_{dp} decomposition peak temperature; ΔH_d the decomposition enthalpy

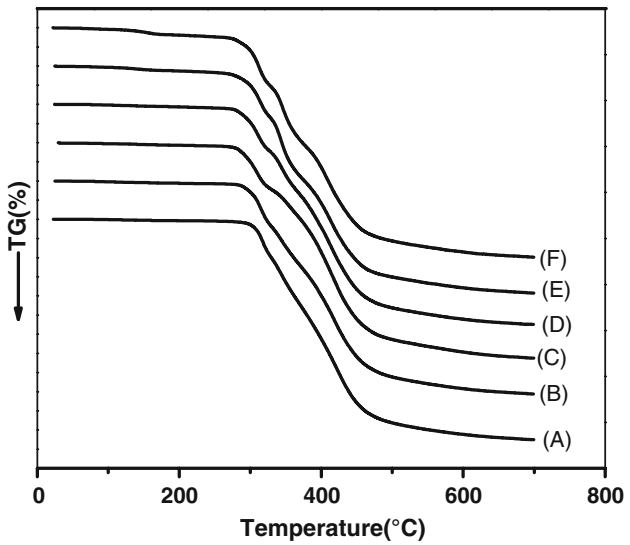

Fig. 6 TG curves of AN–MA (85/15) copolymers containing various contents of MicroPCMs

temperature (5 wt% weight loss) of the copolymers is approximately 300 °C. The copolymers lose weight quickly when the temperature is higher than approximately 310 °C, which corresponds to the decomposition of the copolymer chain as listed in Table 2.

Melting index

The effect of the content of MicroPCMs on MI of the composite is shown in Fig. 7. At the beginning, the microcapsules act as a plasticizer, MI increases with increasing the content of MicroPCMs. When the content of MicroPCMs exceeds 5 wt%, the infusible microcapsules prohibit the molecular chain flow freely, leading to the decrease of MI. MI of the copolymers containing approximately 20 wt% of MicroPCMs drops to the lowest value. Continuously increasing the content of MicroPCMs, the friction between MicroPCMs and cylinder breaks them down, *n*-octadecane is released. The released *n*-octadecane in the copolymers acts as a plasticizer; hence MI increases again. The effect of the content of MicroPCMs on MI of AN–MA copolymer is very similar to that of MicroPCMs in polyethylene [8].

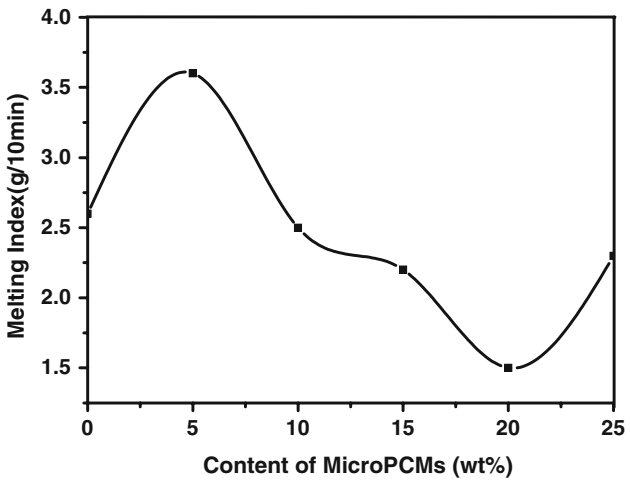

Fig. 7 The effect of the content of MicroPCMs on MI

Morphologies and phase change properties of the fibers

SEM micrographs of AN–MA 85/15 fiber and the fiber containing 20 wt% MicroPCMs are shown in Fig. 8. The side surface of the fiber (a) is very smooth while the fiber containing MicroPCMs (d) is a little coarse. The cross section of the fiber (b, c) is compact. There are a number of MicroPCMs and microporous in the cross section (e, f) of the fiber containing MicroPCMs. The presence of MicroPCMs leads to the formation of microporous structure of fibers. The tensile fracture surface (g) of AN–MA 85/15 fiber is tidiness while that of the fiber containing MicroPCMs is irregular. The phenomenon shows that the structure of the fiber without MicroPCMs is very compact and the structure of the fiber containing MicroPCMs is loose and has defects.

The phase change properties of the thermo-regulated fibers are presented in Fig. 9 and Table 3. The vertical coordinate of Fig. 9 has been translated. As the contents of MicroPCMs increase, the phase change temperature and enthalpies increase gradually. The crystalline enthalpies of the fibers containing 20 and 25 wt% of MicroPCMs are 21 and 25 J/g, respectively. The enthalpy of the fibers containing 10 wt% of MicroPCMs is significantly higher than the expected value 4 J/g by Lennox-Kerr [3]. The efficiency of enthalpy fluctuates at approximately 60% as the content of MicroPCMs changes; and is significantly higher than the literature efficiency value 43% [8]. The decrease of efficiency of enthalpy is related to the percentage of damaged MicroPCMs during the melt-spun processes, the thermal conductivity between polymer and microcapsule, and the thermal conductivity between shell and core of the microcapsule, etc.

The crystallization of the fibers

The X-ray diffraction patterns of the fibers containing various contents of MicroPCMs are shown in Fig. 10. The vertical coordinate of Fig. 10 has been translated. The reflection peak of PAN crystals is located at 16.9° (2θ); and it keeps stable in all the samples, which indicates crystalline form to be same in the fibers containing various contents of MicroPCMs. The relatively low diffraction peak of

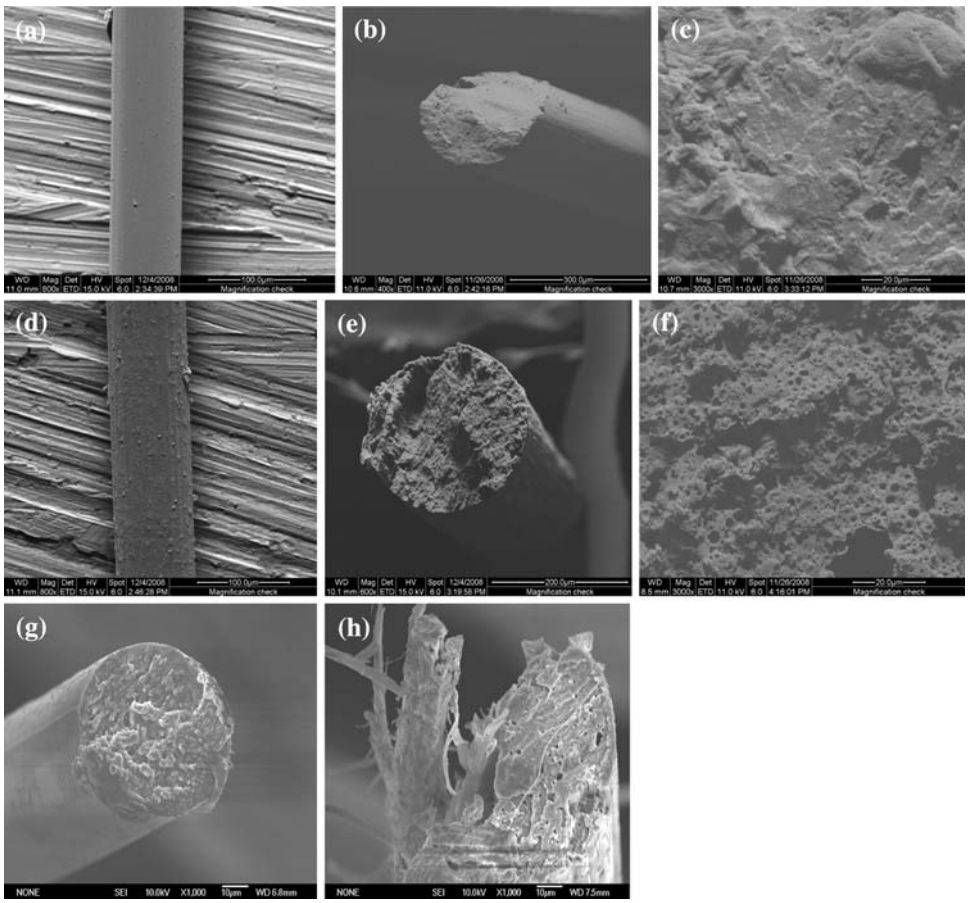

Fig. 8 SEM micrographs of the fibers: **a** AN–MA fiber (×800); **b** freeze-fracture surface, AN–MA fiber (×400); **c** AN–MA fiber (×3000); **d** fiber containing 20 wt% MicroPCMs (×800); **e** freeze-fracture surface, fiber containing 20 wt% MicroPCMs (×400); **f** fiber containing 20 wt% MicroPCMs (×3000); **g** tensile fracture surface, AN–MA fiber (×1000); **h** tensile fracture surface, fiber containing 20 wt% MicroPCMs (×1000)

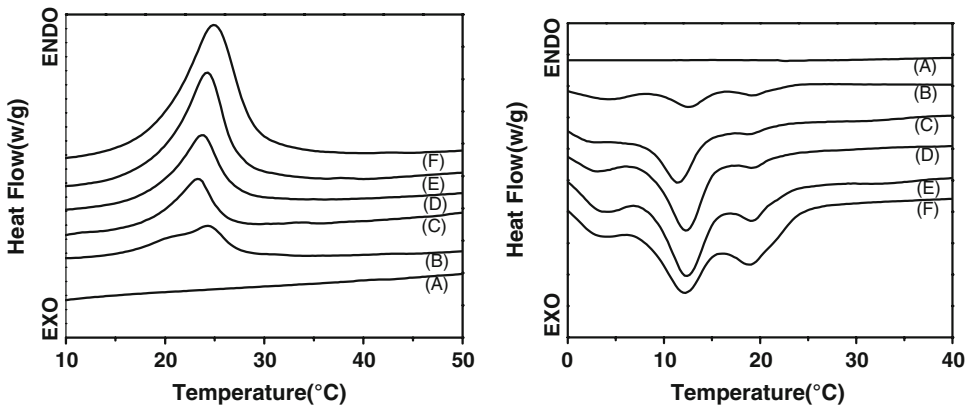

Fig. 9 DSC curves of the thermo-regulated fibers depicting phase change properties: (*A* 0 wt%, *B* 5.1 wt%, *C* 10.2 wt%, *D* 15.3 wt%, *E* 19.8 wt%, *F* 24.9 wt%)

AN–MA (85/15) copolymer fiber corresponds to a low degree of crystallinity. The copolymerization of AN with MA decreases the regularity of PAN chains and thus, reduces the crystallinity of the copolymer. A diffraction peak is also observed at 21.0° (2θ) that may be the contribution of crystals of *n*-octadecane [19]. With increasing the content of MicroPCMs, the intensity of PAN crystallization peak (16.9°) reduces; and the intensity of MicroPCMs crystallization peak (21.0°) increases.

Physical mechanical properties of the fibers

The tensile stress–strain plots for the fibers containing various contents of MicroPCMs are shown in Fig. 11 and Table 4. The tensile strength of AN–MA 85/15 copolymer fiber is equivalent to that reported in literature [14], in which the copolymer was fabricated using emulsion polymerization. The tensile strain of AN–MA 85/15 copolymer fiber is lower than that reported in literature

Table 3 Phase change properties of the thermo-regulated fibers

Sample no.	Efficiency of enthalpy (%)	T_m (°C)		ΔH_m (J/g)	T_c (°C)		ΔH_c (J/g)
		T_{mo}	T_{mp}		T_{co}	T_{cp}	
A	–	–	–	–	–	–	–
B	69.3	14.8	24.2	5	15.2	12.4	7
C	67.3	19.2	23.3	10	14.0	11.3	7
D	48.4	19.2	23.8	11	15.5	12.2	13
E	56.1	19.2	24.2	16	16.2	12.3	21
F	63.0	18.9	24.9	23	16.9	13.2	25
MicroPCMs	100	20.4	27.3	145	24.7	20.2	147

T_{mo} melting starting temperature, T_{mp} melting peak temperature, ΔH_m enthalpy of melting, T_c crystallization temperature on the DSC cooling curve, T_{co} crystallization onset temperature, T_{cp} crystallization peak temperature, ΔH_c enthalpy of crystallization

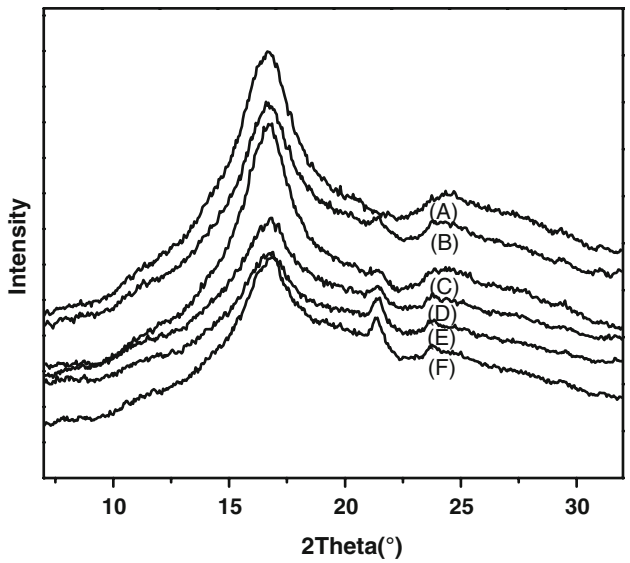

Fig. 10 XRD patterns of the fibers containing various contents of MicroPCMs: (*A* 0 wt%, *B* 5.1 wt%, *C* 10.2 wt%, *D* 15.3 wt%, *E* 19.8 wt%, *F* 24.9 wt%)

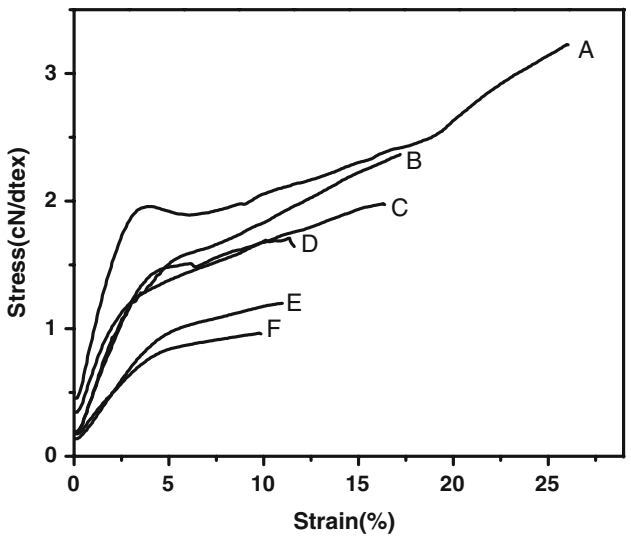

Fig. 11 Stress–strain curves of the fibers containing various contents of MicroPCMs: (*A* 0 wt%, *B* 5.1 wt %, *C* 10.2 wt%, *D* 15.3 wt%, *E* 19.8 wt%, *F* 24.9 wt%)

[14]. The reason needs to be further studied. The tensile strength and elongation decrease with increasing the contents of MicroPCMs. The phenomenon can be explained as that the existence of MicroPCMs brings some defects to the fibers.

Conclusions

AN–MA (85/15) copolymer and the copolymers containing various contents of MicroPCMs were synthesized by aqueous redox initiated polymerization. The copolymer composition agrees well with the feeding ratio of acrylonitrile and methyl acrylate monomers. The AN–MA copolymer and the copolymers containing MicroPCMs were melt spun into fibers at 200 °C. The glass transition temperature (T_g) of the copolymers are in the range of 88.4–91.7 °C; and they increase as the content of MicroPCMs increases. The crystalline enthalpies of the fibers containing 20 and 25 wt% of MicroPCMs are 21 and 25 J/g, respectively. The tensile strength of the fibers is in the range of 1.0–3.2 cN/dtex. Meanwhile, the elongation of the fibers is in the range of 9.9–26.1%. The as-spun PAN-based fiber and that fiber containing 20 and 25 wt% of MiroPCMs exhibit preferable thermoplastic behaviors and thermo-regulated property. This investigation provides a

Table 4 Physical mechanical properties of thermo-regulated AN–MA copolymer fibers

The contents of MicroPCMs in fibers (wt%)	0	5.1	10.2	15.3	19.8	24.9
Tensile strength (cN/dtex)	3.2	2.4	2.0	1.6	1.2	1.0
Elongation (%)	26.1	17.2	16.4	11.6	10.9	9.9

basis for melt-spinning PAN fiber and PAN-based thermo-regulated fiber. Further work on methods of post processing and treatment is in progress.

Acknowledgements The authors are thankful to the National Natural Science Found of China (No. 50573058) and Specialized Research Found for the Doctoral Program of Higher Education (No. 20050058004) for the financial supports.

References

1. Chaurasia PBL (1981) Res Ind 26:159
2. Colvin DP, Mulligan JC (1990) US Patent 4,911,232
3. Lennox-kerr P (1998) Techn Text Int 7:25
4. You M, Zhang XX, Li W et al (2008) Thermochim Acta 472:20
5. Zhang XX, Li Y, Tao XM, Yick KL (2005) Indian J Fiber Textile Res 30:377
6. Bryant YG, Colvin DP (1988) US Patent 4756985
7. Bryant YG (1999) In: American Society of Mechanical Engineers, Bioengineering Division BED Advances in Heat and Mass Transfer in Biotechnology, Nashville, TN, USA, 14–19 November
8. Zhang XX, Wang XC, Tao XM et al (2005) J Mater Sci 40:3729. doi:10.1007/s10853-005-3314-8
9. Zhang XX, Fan YF, Tao XM et al (2004) Mater Chem Phys 88(2–3):300
10. Zhang XX, Tao XM, Yick KL et al (2006) Text Res J 76:351
11. Clarke AJ, Bailey JE (1973) Nature 243:146
12. Mukundan T, Bhanu VA, Wiles KB et al (2006) Polymer 47:4163
13. Bhanu VA, Rangarajan P, Wiles K et al (2002) Polymer 43:4841
14. Hutchinson SR, Tonelli AE, Gupta BS et al (2008) J Mater Sci 43:5143. doi:10.1007/s10853-008-2727-6
15. Han N, Zhang XX, Wang XC (2007) Polym Mater Sci Eng 23:45
16. Rangarajan P, Yang J, Bhanu V et al (2002) J Appl Polym Sci 85:69
17. Fan YF, Zhang XX, Wu SZ et al (2005) Thermochim Acta 429:25
18. Zhang XX, Tao XM, Yick KL, Wang XC (2004) Colloid Polym Sci 282:330
19. Li J, Han N, Zhang XX (2006) J Donghua Univ (Eng Ed) 23:10